# An Evaluation of the Accuracy of Some Radar Wind Profiling Techniques

ALBERT J. KOSCIELNY, RICHARD J. DOVIAK AND DUSAN S. ZRNIC'

*National Severe Storms Laboratory, Norman, OK 73069*

(Manuscript received 24 February 1984, in final form 2 August 1984)

ABSTRACT

Advances in clear air Doppler radar measurement have made practical the monitoring of radial velocities in the troposphere and lower stratosphere and even the vector wind, under some assumptions. Because the objective of wind profiling is to monitor winds representative of larger scale atmospheric motions, an assumption of a time-invariant spatially uniform wind field is commonly used. Then, the accuracy of the wind estimators depends on the error variance of the radial velocity, the departure from uniformity of the wind field and the measurement geometry.

We derive expressions for the variance and bias for some of these estimators when applied to a spatially linear wind field. The techniques we consider are three fixed beams, azimuthal scanning (VAD) and elevation scanning (VED). In addition, we examine a method based on the integration of the continuity equation to estimate the areal-averaged wind. This technique sometimes leads to better estimates than do direct methods.

## 1. Introduction

Major advances in Doppler radar measurement in optically clear air have made it feasible to monitor radial velocities in the troposphere and lower stratosphere (see, e.g., Balsley and Gage, 1982). However, for most applications we wish to deduce the wind vector from these radial velocities. Measurement of the wind vector with a single radar can be made assuming a spatially uniform, time invariant wind field. The components of the wind are estimated by the parameters of a linear regression of the radial velocities on functions of their spatial locations so that the accuracy of the wind estimate depends on the locations of the radial velocity measurements.

As noted by Peterson and Balsley (1979), a trade-off exists for a given technique between the accuracies of horizontal and vertical wind component measurements. Because we usually need to measure each of the three components of wind with different accuracy and as inexpensively as possible, we are led to evaluate the efficiency of some of the common retrieval techniques. The techniques we will consider are the three fixed beams, azimuthal scanning (VAD) and elevation scanning (VED).

## 2. Error analysis theory

Estimation of parameters of a linear wind field from radial velocities is discussed by several authors, e.g., Browning and Wexler (1968), Waldteufel and Corbin (1979) and Koscielny *et al.* (1982). The measured radial velocity $v_r$ can be modeled by a linear regression equation of the form

$$v_r = \mathbf{P}_m \mathbf{K}_m + \epsilon, \tag{1}$$

where $\mathbf{P}_m$ is a row vector of regressor variables, which are functions of range $r$, azimuth $\phi$ and elevation angle $\theta_e$; $\mathbf{K}_m$ is a column vector of $m$ parameters of the linear wind field. The errors $\epsilon$ may be due to nonuniform reflectivity, turbulence, targets such as hydrometeors that move relative to the wind, and a nonlinear wind. As shown by Draper and Smith (1981, p. 87) least-squares estimates of $\mathbf{K}_m$ are computed from $n$ measurements of $v_r$ by

$$\hat{\mathbf{K}}_m = (\mathbf{P}_{nm}^T \mathbf{P}_{nm})^{-1} (\mathbf{P}_{nm}^T \mathbf{V}_n), \tag{2}$$

where superscript $^T$ indicates transpose and $\mathbf{P}_{nm}$ is an $n \times m$ matrix of the regressor variables corresponding to the $n$ radial velocity measurements in $\mathbf{V}_n$. Measurement errors in the radial velocities produce uncertainties in the estimate $\hat{\mathbf{K}}_m$ (see Draper and Smith, p. 89), and the covariances of $\hat{\mathbf{K}}_m$ about $\mathbf{K}_m$ are given by

$$\mathbf{C}_{mm} = (\mathbf{P}_{nm}^T \mathbf{P}_{nm})^{-1} \sigma_\epsilon^2, \tag{3}$$

where $\sigma_\epsilon^2$ is the variance of $\epsilon$.

If the wind field has variations not modeled by (1), the $\hat{\mathbf{K}}_m$ will be biased (Draper and Smith, p. 113); the amount of bias $\mathbf{B}_m$ is given by the product of a known alias matrix $\mathbf{A}_{ml}$ with the vector $\mathbf{K}_l$ of the $l$ unknown parameters of the wind field not included in $\mathbf{K}_m$. Thus,

$$\mathbf{B}_m = \mathbf{A}_{ml} \mathbf{K}_l, \tag{4}$$

where

$$\mathbf{A}_{ml} = (\mathbf{P}_{nm}^T \mathbf{P}_{nm})^{-1} (\mathbf{P}_{nm}^T \mathbf{P}_{nl}). \tag{5}$$

Here, $\mathbf{P}_{nl}$ is a matrix of regressor variables for the components not included in (1).

The various techniques referred to in the Introduction assume the wind to be uniform (i.e., the first

and higher order derivatives are zero) over the data analysis volume. We propose to analyze the errors in these techniques by computing the bias and variance of the least-squares estimates $\hat{\mathbf{K}}_m$ with the assumptions that $\sigma_\epsilon^2$ is constant at a given range and the wind field is actually linear. Thus, $m = 3$ and $\mathbf{K}_3$ contains the three uniform components ($u_0$, $v_0$, $w_0$), and $l = 8$ so $\mathbf{K}_8$ contains the eight spatial derivatives ($u_x$, $u_z$, $v_y$, $v_z$, $u_y + v_x$, $w_x$, $w_y$, $w_z$) of the linear wind. Horizontal vorticity cannot be determined from single Doppler data and as discussed by Waldteufel and Corbin (1979), the derivatives $u_y$ and $v_x$ appear only in a sum term. In our evaluation and comparison of techniques, we assume that a total of $n$ measurements are available for each and that these $n$ measurements are distributed in space at constant height $h$.

### a. Fixed beam

We consider a configuration for the fixed beam technique in which three beams, one vertical and two off-vertical at elevation $\theta_e$, are sampled. The off-vertical beams usually have perpendicular horizontal projections; for convenience, we will consider them to have azimuths 0 and 90°. The total number of radial velocity measurements for a height $h$ for all three beams is $n$; for generality, we let the number of vertical measurements be $N$.

The bias and variance properties of the estimates $\hat{\mathbf{K}}_3^T = (\hat{u}_0, \hat{v}_0, \hat{w}_0)$ are computed in Appendix A using (3) and (5), and we find that, for $n = 3N$,

$$\mathrm{VAR}(\hat{u}_0) = \mathrm{VAR}(\hat{v}_0) = \frac{\sigma_\epsilon^2}{n} 3(\sec^2\theta_e + \tan^2\theta_e),$$

$$\mathrm{VAR}(\hat{w}_0) = \frac{\sigma_\epsilon^2}{n} 3, \tag{6}$$

$$\mathrm{bias}\begin{bmatrix}\hat{u}_0\\ \hat{v}_0\\ \hat{w}_0\end{bmatrix} \approx h\begin{bmatrix}u_x\cot\theta_e + w_x\\ v_y\cot\theta_e + w_y\\ 0\end{bmatrix}. \tag{7}$$

The bias equation is approximate because we have used $h \approx r\sin\theta_e$, which is appropriate for $r \leq 30$ km. From (7) we see that the bias due to spatial derivatives is a linear function of height, which is expected because the beam separation is linearly dependent on $h$. In addition, we see from (6) and (7) that the variance decreases with $n$, but that the bias cannot be reduced by data averaging.

### b. Azimuthal scanning

In an azimuthal scanning technique, usually called VAD (Velocity Azimuth Display), data along a circle centered on the radar are used to estimate directly the components of the uniform wind field. The results of the variance and bias equation evaluation, given in Appendix B, are

$$\mathrm{VAR}(\hat{u}_0) = \mathrm{VAR}(\hat{v}_0) = \frac{\sigma_\epsilon^2}{n} \times 2\sec^2\theta_e, \tag{8a}$$

$$\mathrm{VAR}(\hat{w}_0) = \frac{\sigma_\epsilon^2}{n} \times \csc^2\theta_e, \tag{8b}$$

$$\mathrm{bias}\begin{bmatrix}\hat{u}_0\\ \hat{v}_0\\ \hat{w}_0\end{bmatrix} \approx h\begin{bmatrix}w_x\\ w_y\\ \frac{1}{2}(u_x + v_y)\cot^2\theta_e\end{bmatrix}. \tag{9}$$

### c. Elevation scanning

In the elevation scanning VED (Velocity Elevation Display) technique, radial velocities at height $h$ are collected for elevation angles $\theta_0 \leq \theta_e \leq \pi - \theta_0$. We assume $n/2$ data are collected for the two azimuths 0 and 90°; therefore, both horizontal components are measured. Appendix C shows

$$\mathrm{VAR}(\hat{u}_0) = \mathrm{VAR}(\hat{v}_0) = \frac{\sigma_\epsilon^2}{n} \times \frac{4(\pi - 2\theta_0)}{\{\pi - 2\theta_0 - \sin(\pi - 2\theta_0)\}},$$

$$\mathrm{VAR}(\hat{w}_0) = \frac{\sigma_\epsilon^2}{n} \times \frac{2(\pi - 2\theta_0)}{\{\pi - 2\theta_0 + \sin(\pi - 2\theta_0)\}}, \tag{10}$$

$$\mathrm{bias}\begin{bmatrix}\hat{u}_0\\ \hat{v}_0\\ \hat{w}_0\end{bmatrix} \approx h\begin{bmatrix}w_x\\ w_y\\ (u_x + v_y)\left[\dfrac{\pi - 2\theta_0 - \sin(\pi - 2\theta_0)}{\pi - 2\theta_0 + \sin(\pi - 2\theta_0)}\right]\end{bmatrix}. \tag{11}$$

## 3. Comparison of the techniques

Our analysis results for the variance and bias of the uniform wind estimates are summarized in Table 1. The variances all depend on the product of $\sigma_\epsilon^2/n$, with a geometric factor specific to each technique. The geometric factors are functions of elevation angle $\theta_e$ for the three fixed beams and VAD, and of the elevation angle interval $2\pi - 2\theta_0$ for VED. The biases depend on the product of the height $h$ and some combination of the unknown spatial derivatives. Since it is difficult to make a direct error comparison of the various techniques, we propose to compare variances through a quantity we will call efficiency. We compare biases by evaluating the bias equation for each technique at the same height and using identical values of the spatial derivatives.

### a. Efficiency

Because these techniques produce uniform wind estimates with differing variances, a standard for their

TABLE 1. Variance and bias equations for horizontal and vertical wind estimates obtained from fixed beam, azimuth scanning or elevation scanning techniques. $\mathrm{VAR}(\hat{v}_0) \equiv \mathrm{VAR}(\hat{u}_0)$, and for Bias $(\hat{v}_0)$ replace $u$ with $v$ and $x$ subscript with $y$.

| | Fixed beam (one vertical) | Azimuth scanning (VAD) | Elevation scanning (VED) |
|---|---|---|---|
| $\mathrm{VAR}(\hat{u}_0)$ | $\frac{\sigma_\epsilon^2}{n} 3(\sec^2\theta_e + \tan^2\theta_e)$ | $\frac{\sigma_\epsilon^2}{n} 2\sec^2\theta_e$ | $\frac{\sigma_\epsilon^2}{n} 4\left[\frac{\pi - 2\theta_0}{(\pi - 2\theta_0) - \sin(\pi - 2\theta_0)}\right]$ |
| $\mathrm{VAR}(\hat{w}_0)$ | $\frac{\sigma_\epsilon^2}{n} 3$ | $\frac{\sigma_\epsilon^2}{n} \csc^2\theta_e$ | $\frac{\sigma_\epsilon^2}{n} 2\left[\frac{\pi - 2\theta_0}{(\pi - 2\theta_0) + \sin(\pi - 2\theta_0)}\right]$ |
| $\mathrm{Bias}(\hat{u}_0)$ | $h(u_x \cot\theta_e + w_x)$ | $hw_x$ | $hw_x$ |
| $\mathrm{Bias}(\hat{w}_0)$ | 0 | $h(u_x + v_y)\frac{\cot^2\theta_e}{2}$ | $h(u_x + v_y)\left[\frac{\pi - 2\theta_0 - \sin(\pi - 2\theta_0)}{\pi - 2\theta_0 + \sin(\pi - 2\theta_0)}\right]$ |

performance is needed. They can be viewed as estimators (in the statistical sense) of the uniform wind parameters ($u_0$, $v_0$, $w_0$). The ratio of the variance $V_{\min}$ of the best possible estimator to the variance of a given estimator is termed the efficiency $E$ of the estimator (see, e.g., Afifi and Azen, 1972, p. 315). The variance of a wind component estimate at a constant height $h$ will depend on several parameters (i.e., the elevation angle or interval, spectrum width, signal to noise ratio), some of which are functions of the range $r$ to the measurement location. If the range is fixed, the minimum variance occurs in the (not necessarily realizable) situation when the component is collinear with the radar beam. Therefore, a best estimate of a horizontal component at height $h$ would be made if a radar located at that height were to measure directly the desired horizontal component. To make the comparisons meaningful, the measurement would have to be made at least a distance $h$ from the radar. We chose $r = h$ as a standard for comparison because, with the above caveat, it leads to minimum variance: $V_{\min} = \sigma_\epsilon^2(h)/n$. For example, the efficiency at range $r$ of $\hat{u}_0$ estimated by the fixed beam technique would be

$$E = V_{\min}/\mathrm{VAR}(\hat{u}_0) = \sigma_\epsilon^2(h)/\sigma_\epsilon^2(r)[3(\sec^2\theta_e + \tan^2\theta_e)].$$

The variance $\sigma_\epsilon^2$ of the radial velocities has two principal contributors. The deviations about the uniform wind due to turbulence on scales larger than the radar resolution volume will be characterized by an uncertainty of variance $\sigma_m^2$ where the subscript $m$ indicates its meteorological origin. The statistical uncertainty due to receiver noise and turbulence scales smaller than the radar resolution volume are characterized by the variance $\sigma_{\hat{v}}^2$. Thus,

$$\sigma_\epsilon^2 = \sigma_{\hat{v}}^2 + \sigma_m^2. \tag{12}$$

Because clear air echoes have low signal-to-noise ratios (SNR), $\sigma_{\hat{v}}^2$ is primarily a function of SNR if spectrum width is small compared to the Nyquist velocity (Zrnic', 1979). But SNR depends on the inverse square of range $r$ (Doviak and Zrnic', 1984) so at constant height and for a uniformly filled resolution volume,

$$\sigma_{\hat{v}}^2 = b_1\,\mathrm{SNR}^{-2} = br^4 \approx bh^4\csc^4\theta_e, \tag{13}$$

where $b$ is a proportionality constant, and the approximation $r \approx h\sin\theta_e$ has been used. The effects of beam refraction and earth's curvature for typical profiling geometries are insignificant and have not been incorporated in (13). We assume $\sigma_m^2$ is horizontally isotropic but can vary with height. Thus,

$$\frac{\sigma_\epsilon^2}{n} = \frac{bh^4\csc^4\theta_e + \sigma_m^2}{n}, \tag{14}$$

$$V_{\min} = (\sigma_m^2 + bh^4)/n. \tag{15}$$

The efficiency of the fixed beam technique, for example, can be expressed as

$$E = 3\eta(\sec^2\theta_e + \tan^2\theta_e),$$

where

$$\eta = \frac{\sigma_m^2/bh^4 + 1}{\sigma_m^2/bh^4 + \csc^4\theta_e}. \tag{16}$$

The efficiencies for the other techniques can also be expressed as the product of $\eta$ and some function (particular to the technique) of elevation angle. Hence, $\eta$, which we will call the efficiency factor, provides a quantitative measure of variance degradation common to the three techniques. The common degradation depends on the meteorological variance and signal-to-noise ratio and, because measurements are at a constant height, the SNR is expressed in terms of $h$ and $\theta_e$.

A short discussion on the values of $\sigma_m^2/bh^4$ is in order. It has been our experience that turbulence in the planetary boundary layer places a lower bound on $\sigma_m^2$ of about 1 $\mathrm{m^2\ s^{-2}}$ (see Rabin and Zrnic', 1980, Fig. 6, or Doviak and Berger, 1980, Table 2a). However, smaller values at higher altitudes cannot be excluded. The variance due to receiver noise $bh^4$ can be insignificant if echoes have sufficient strengths, but for regions of weak echoes it may be substantial. For example, a 6 m wavelength radar will have radial velocity error variances exceeding 1 $\mathrm{m^2\ s^{-2}}$ if the SNR is less than $-10$ dB (dwell times are less than 2 minutes, Doppler spectrum width is 1 $\mathrm{m\ s^{-1}}$ and

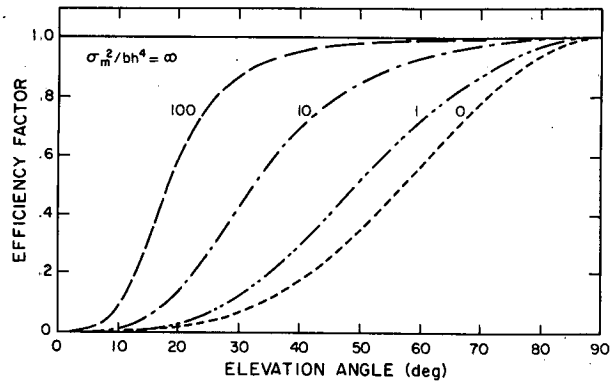


FIG. 1. Efficiency factor for selected values of $\sigma_m^2/bh^4$.

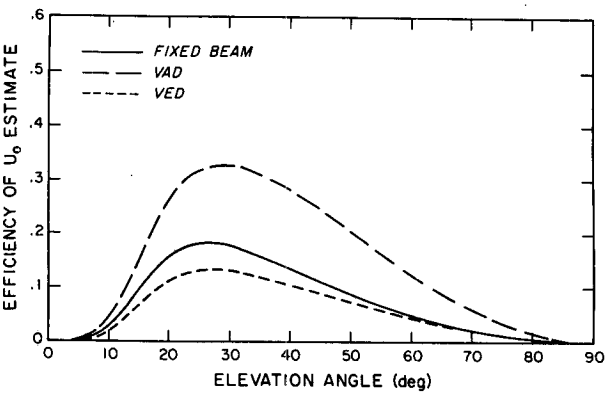


FIG. 3. As in Fig. 2 but for $\sigma_m^2/bh^4 = 100$.

time samples for Doppler processing are spaced 0.1 s apart). So it is reasonable to examine the efficiencies for $\sigma_m^2 \gg bh^4$, $\sigma_m^2 = bh^4$ and $\sigma_m^2 \ll bh^4$.

The efficiency factor for selected ratios of the meteorological variance to noise-induced variance, $\sigma_m^2/bh^4$, is plotted in Fig. 1. It increases toward 1 as $\theta_e$ increases; for $\sigma_m^2 \gg bh^4$, $\eta$ reaches 1 very quickly, showing that when meteorological variance is dominant, the efficiency factor is nearly independent of $\theta_e$ and $h$. For the case $\sigma_v^2 = 0$ the efficiency in estimating horizontal components is given as in Fig. 2, where we see that the VAD technique has the highest efficiency for all elevation angles. In addition, VAD maintains reasonable efficiency to larger elevation angles (75°) than either fixed beam or VED.

Figures 3 and 4 show the efficiencies for $\sigma_m^2/bh^4 = 100$ and $\sigma_m^2/bh^4 \to 0$. Changes in $\sigma_m^2/bh^4$ do not permute the efficiency curves with respect to each other since $\eta$ is the same for all. However, because the measurement is at constant height, data from closer ranges have lower variance so the peaks of the curves shift from zero to larger elevation angles. The case $\sigma_m^2 = bh^4$ (not shown) is very similar to $\sigma_m^2 = 0$, except that the peaks are at 50°.

The efficiencies of the vertical velocity estimates for the case $\sigma_v^2 = 0$ are shown in Fig. 5. It is not surprising that the VED has the highest efficiency, because it obtains most measurements near vertical incidence, but for large elevation angles, the VAD is comparable. The fixed beam has a constant efficiency of ⅓ since the number of vertical estimates is fixed at $n/3$. When the relative contribution of noise variance to $\sigma_\epsilon^2$ increases (i.e., $\sigma_m^2/bh^4$ decreases), the efficiency factor decreases (Fig. 1) and the efficiencies become lower as can be seen in Fig. 6.

### b. Bias

Because the estimate biases depend linearly on the height $h$, we so compare the bias per unit height that the bias for other heights can be computed easily. The biases depend on the value of unknown spatial derivatives. Following Waldteufel and Corbin (1979) we use $u_x = v_y = 10^{-3}$ s$^{-1}$ and $w_x = w_y = 10^{-4}$ s$^{-1}$ as maximum values. The biases thus computed are shown in Fig. 7 for the horizontal components and in Fig. 8 for the vertical component. The asymmetry of the beam locations about the vertical for the fixed beam technique produces a horizontal wind bias due to $u_x$ and $v_y$, which decreases as $\cot\theta_e$. The biases due to $u_x$ and $v_y$ can be removed if $u_0$ and $v_0$ are

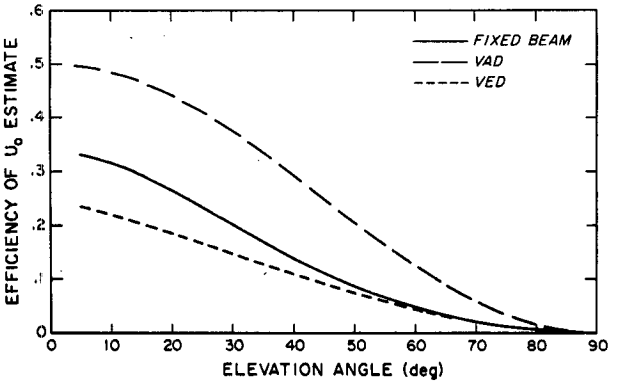


FIG. 2. Variation of horizontal wind estimator efficiencies with elevation angle and for $\sigma_v = 0$.

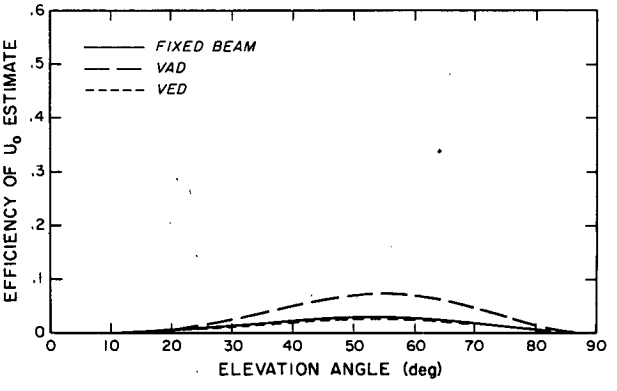


FIG. 4. As in Fig. 2 but for $\sigma_m^2 = 0$.

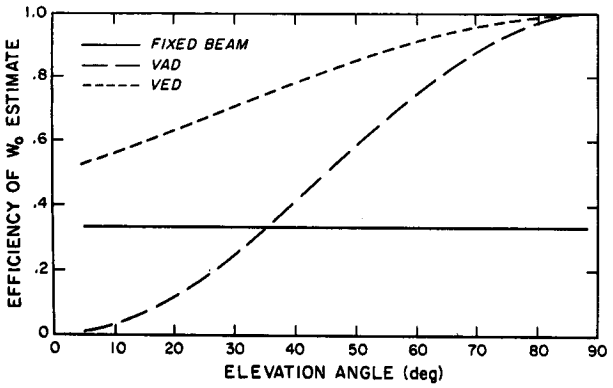


FIG. 5. Variation of vertical wind estimator efficiencies with elevation angle for $\sigma_v^2 = 0$.

placed at ($r \cos\theta_e$, 0) and (0, $r \cos\theta_e$), respectively. The bias then equals the VAD biases but the $u_0$, $v_0$ estimates are no longer collocated. For simplicity, we have chosen to analyze the collocated estimates. The horizontal wind biases for the VAD and VED are the same and are constant with elevation angle. For the fixed beam technique, the vertical velocity is not biased by any derivatives. The vertical wind bias in the VED and VAD decreases with increasing elevation angle.

### c. Error comparison summary

Although the variance for horizontal components increases as $\theta_e \rightarrow 90°$, it can be controlled to an extent by data averaging. The vertical velocity variance and the bias errors can be decreased by using larger elevation angles. Because bias increases with height, the higher altitudes may require a vertical measurement for vertical velocity. Furthermore, scattering from anisotropic irregularities may prevail at vertical incidence giving rise to enhanced echo power and a consequent increase in SNR (Doviak and Zrnic' 1984). Whereas this tends to improve measurements of vertical velocities, it is important to bear in mind that when the beam is pointed straight up the magnitude of Doppler shifts will, in general, be smallest. This would put Doppler spectral peaks of clear air echoes very close to zero, where they may be masked by ground clutter returns through the antenna sidelobes.

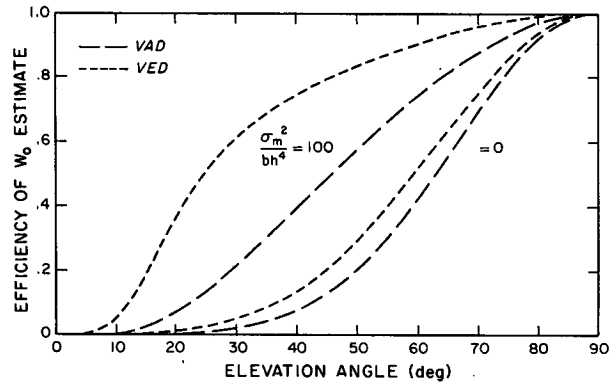


FIG. 6. As in Fig. 5 but for different ratios $\sigma_m^2/bh^4$.

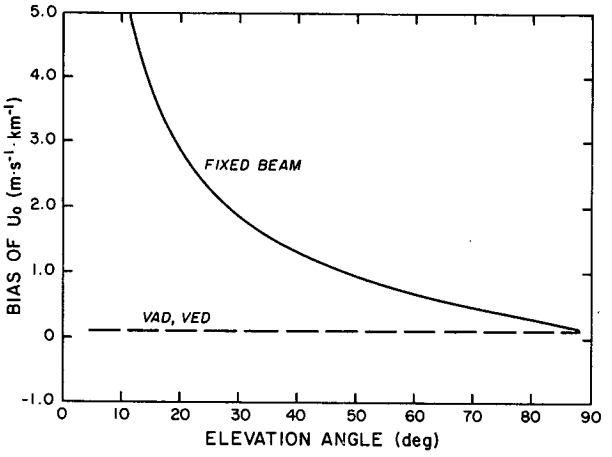


FIG. 7. Horizontal wind estimator bias error per unit height with $u_x = v_y = 10^{-3}$ s$^{-1}$, $w_x = w_y = 10^{-4}$ s$^{-1}$. VAD and VED biases overlap.

### d. Example

The bias and variance equations can be used to choose an elevation angle for profiling. For example, suppose we wish to profile the winds at 5 km using 360 measurements and let $\sigma_\epsilon = 1$ m s$^{-1}$ be entirely due to meteorological contributions. The square root of the mean square errors (bias squared plus variance) for the horizontal and vertical components are shown in Figs. 9 and 10 for each of the techniques. We have kept vertical and horizontal errors separate because vertical velocity requires greater accuracy. If we require horizontal and vertical velocity accuracies of 1 and

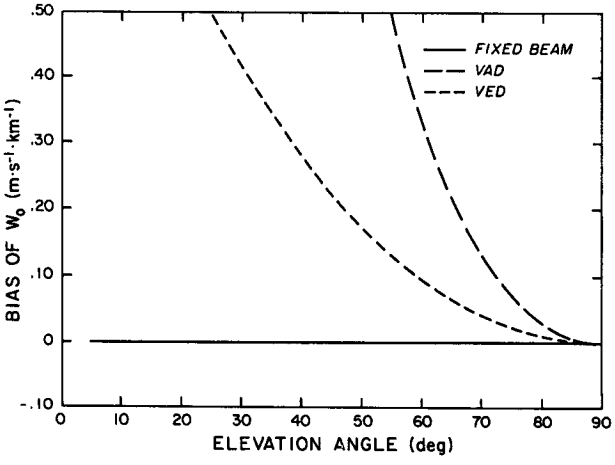


FIG. 8. Vertical wind estimator bias error per unit height with $u_x = v_y = 10^{-3}$ s$^{-1}$, $w_x = w_y = 10^{-4}$ s$^{-1}$.

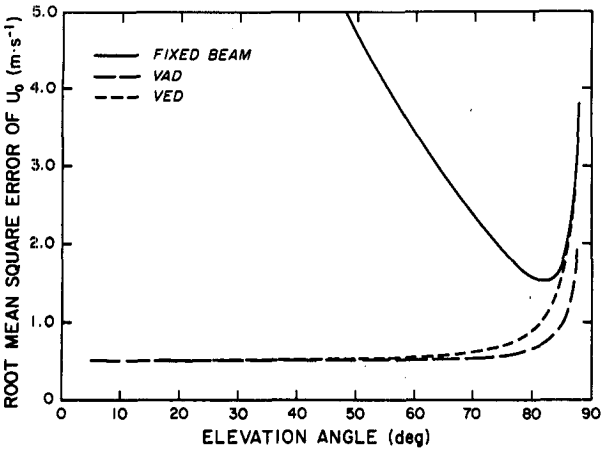


FIG. 9. Root-mean-square error for the horizontal estimator if $\sigma_\epsilon$ = 1 m s$^{-1}$, $n$ = 360, $u_x = v_y = 10^{-3}$s$^{-1}$, $w_x = w_y = 10^{-4}$s$^{-1}$ and $h$ = 5 km.

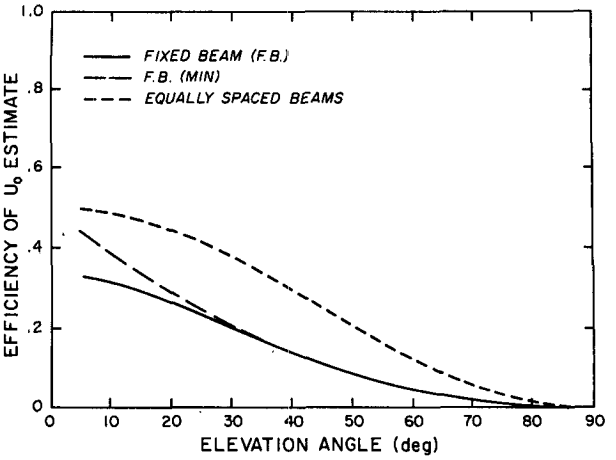


FIG. 11. Horizontal wind estimator efficiency for fixed beam, fixed beam with horizontal error minimization and fixed beam with equally spaced, off-vertical beams.

0.1 m s$^{-1}$, respectively, we would use an elevation angle between 83 and 85° for the VAD and between 77 and 81° for the VED. Because of the bias error, the fixed beam horizontal wind error is 1.5 m s$^{-1}$ or larger (see Fig. 9).

## 4. Possible improvements

In the previous section we have restricted our attention to the simultaneous measurement of the horizontal and vertical wind components, since such measurement techniques are easy to implement. However, some circumstances may require separate measurements for the horizontal and vertical components. Although direct measurements of vertical velocity are intuitively appealing, ground clutter can make estimation difficult since vertical velocities are relatively close to zero (compared to the horizontal velocities). We therefore examine some simple improvements to the techniques analyzed in the previous section, as well as a technique based on the divergence theorem.

### a. *Fixed beam with error minimization*

The wind estimate efficiencies for the fixed beam technique can be improved slightly by collecting an optimum number $N$ of vertical data. Minimizing the first diagonal element of the matrix in (A1.1), which determines the VAR($\hat{u}_0$) and VAR($\hat{v}_0$), gives

$$\frac{N}{n} = \frac{\sin\theta_e}{\sqrt{2} + \sin\theta_e}, \tag{17}$$

so $N$ would vary from $n/3$ at $\theta_e$ = 45° to about 0.4$n$ for $\theta_e$ near 90°. The efficiencies (for $\sigma_{\hat{v}}^2 = 0$) are shown in Fig. 11 for $\hat{u}_0$ and in Fig. 12 for $\hat{w}_0$. It can be seen that for $\theta_e > 45°$, the efficiency of estimating $\hat{u}_0$ is unchanged, but is slightly improved for $\hat{w}_0$.

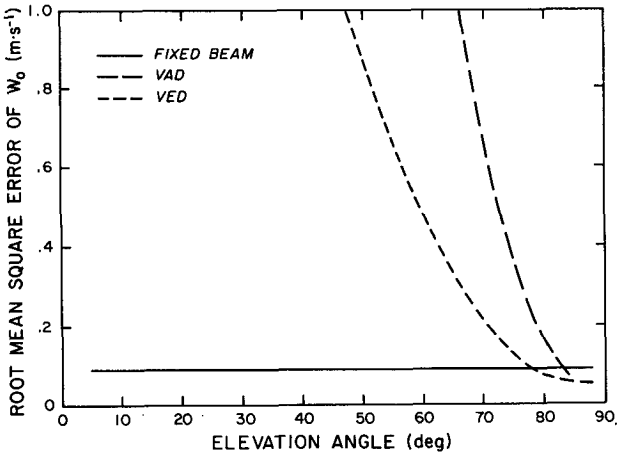


FIG. 10. Root-mean-square error for the vertical estimator if $\sigma_\epsilon$ = 1 m s$^{-1}$, $n$ = 360, $u_x = v_y = 10^{-3}$s$^{-1}$, $w_x = w_y = 10^{-4}$s$^{-1}$ and $h$ = 5 km.

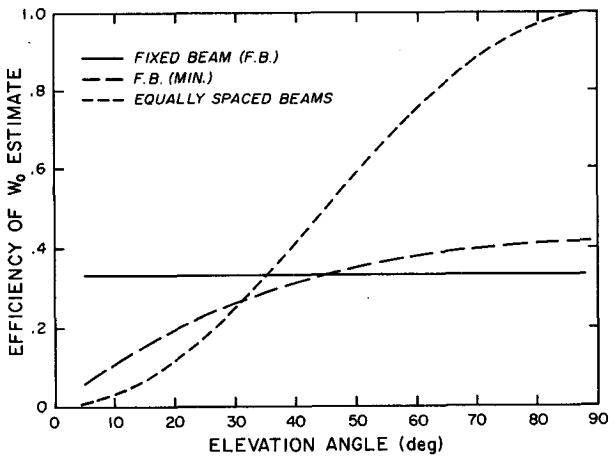


FIG. 12. Vertical wind estimator efficiencies for the same techniques as described in Fig. 11.

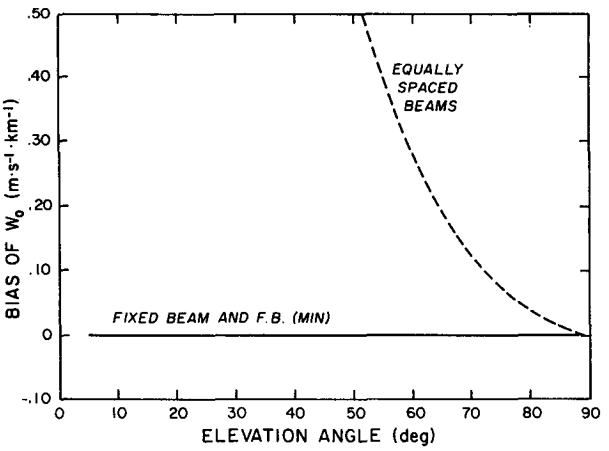


FIG. 13. Vertical wind biases per unit height for the same techniques described in Fig. 11.

As was shown in (6), VAR($\hat{u}_0$) has two terms. The second term, $\sigma_\epsilon^2 \tan^2\theta_e/N$, is the result of removing the vertical velocity bias from $\hat{u}_0$ by a vertical velocity estimate $\hat{w}_0$, with VAR($\hat{w}_0$) = $\sigma_\epsilon^2/N$. The size of the variance contribution from the vertical velocity bias removal appears to indicate that it might be better to ignore the bias error ($w_0 \tan\theta_e$). However, for observation time intervals of several minutes, a mesoscale value of $w_0$ should be used (see Larsen and Röttger, 1982). Thus, for large elevation angles ($\theta_e \geq 75°$), the bias error could be several meters per second. For tropospheric observation under all conditions, the bias should be removed if a horizontal velocity accuracy of 1 m $s^{-1}$ is required.

### b. *Off-vertical fixed beams*

To mitigate ground clutter contamination of vertical velocity estimates, a fixed beam system can have all beams off-vertical at some elevation angle $\theta_e$ so cancelers can better filter the ground clutter affecting the estimation of radial velocity. An analysis of such a system with three beams (see Part (b) of Appendix A) shows that the variances (and efficiencies) of the estimates are identical to those for the VAD technique (cf. Figs. 2 and 5 with Figs. 11 and 12). The bias for the $u_0$ estimate is very similar to the fixed beam with one vertical, but the $w_0$ estimate is biased as shown in Fig. 13.

### c. *Application of the continuity equation to VAD data*

Vertical winds as small as a few centimeters per second are important in forecasting and, as noted earlier, $w_0$ should be estimated with more accuracy than the horizontal components. By applying the mass continuity equation, the vertical wind, averaged over the circle of measurement, can be estimated with good precision. When mass continuity is applied, we will call the technique indirect, whereas the previously discussed techniques (e.g., VAD) are direct measurements of $w$.

Vertical soundings can be made by varying $\theta_e$ and/or $r$. However, because the horizontal area for which $w_0$ is representative varies with $r$, we prefer to keep $r$ constant. Divergence is estimated by applying Gauss's theorem to the volume $V$ (see Fig. 14) enclosed by the area $S_1$ at constant range from the radar and the area $S_2$ at constant height. Applying mass continuity and integrating gives an areal averaged $\bar{w}$, i.e.,

$$\bar{w} = \frac{-2e^{\Gamma h}}{(1 - h^2/r^2)r} \int_0^h e^{\Gamma h} C_0(h) dh, \tag{18}$$

where $\Gamma$ is average lapse rate of air density versus height, and

$$C_0(h) = \frac{1}{2\pi r} \int_0^{2\pi} v_r r d\phi \tag{19}$$

is the average radial velocity around the circle of measurement.

To fix the total number of measurements at $M$, we assume $n$ values of $v_r$ are made on each of $L$ circles (i.e., $M = nL$) spaced at intervals $\Delta h$ from $h = 0$ to $h = h_m$. Then,

$$\hat{C}_0(h) = \frac{1}{n} \sum_{m=1}^{n} \hat{v}_{rm}. \tag{20}$$

If all the radial velocities are independent with the same uncertainty,

$$\text{VAR}(\bar{w}) = \frac{4h^2\sigma_\epsilon^2}{r^2(1 - h^2/r^2)^2 M} \left\{\frac{e^{2\Gamma h} - 1}{2\Gamma h}\right\}, \tag{21}$$

(21) shows, for a fixed $r$, that the variance of $\bar{w}$ becomes larger as the height at which $\bar{w}$ is estimated increases. In contrast, the variance of $\hat{w}_0$ estimated directly by the VAD method [i.e., Eq. (8)] decreases as height increases if $r$ is constant. This decrease in variance results from a larger proportion of the vertical velocity contributing to the radial velocity as $\theta_e$ approaches 90°.

In order to make a more definitive comparison between the direct and indirect VAD methods we consider two cases: 1) a direct VAD where $\theta_e$ is fixed and measurements are made at various ranges to

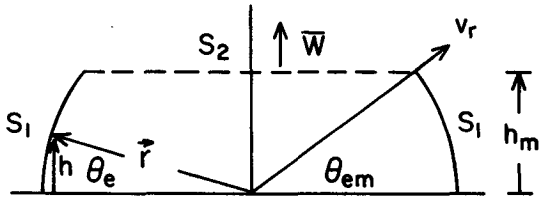


FIG. 14. Geometry to estimate vertical velocity averaged over the circular area $S_2$.

sound the wind at different heights and 2) a direct VAD in which the range is fixed to the value equal to that used in the previously described indirect VAD method. For all three techniques we assume that: $\sigma_m^2$ is larger than $bh^4$; the number $n$ of measurements made at each altitude is the same; the number $L$ of height increments between 0 and the maximum altitude $h_m$ is equal and; $h_m$ = 10 km.

The optimum angle for estimating $u_0$ and $v_0$ depends upon the ratio $\sigma_m^2/bh^4$. For a change in ratio from 0 to 100 (see Figs. 3 and 4), the optimum $\theta_e$ changes from 55 to ~30°. We assume that the radar is designed to keep the variance due to receiver noise less than that due to meteorological effects, so that the ratio will be larger than unity and, hence, optimum elevation angle $\theta_{em}$ will be less than 55°. We assume a $\theta_{em}$ of 45°, which corresponds to an optimum angle when $\sigma_m^2/bh_m^4 = 4$.

The horizontal velocity variance for all three techniques (i.e., the two direct VAD and the indirect VAD methods) is obtained from (8a). This variance, normalized to $4\sigma_m^2/M$, is plotted in Fig. 15 as a function of height $h$. The VAR($\hat{u}_0$) for the direct and indirect VAD methods is the same when $r$ is a constant, and the difference of variances for $\hat{u}_0$ when $\theta_e$ is a constant is negligible.

We apply (8b) to case 1) to obtain the vertical velocity variance for the direct method:

$$\text{VAR}(\hat{w}_0) = \frac{4\sigma_m^2 L}{2M}\left\{1 + \left(\frac{h}{h_m}\right)^4\right\}; \quad \text{constant } \theta_e = 45°. \tag{22}$$

For case 2), where $r = h_m\sqrt{2}$, the application of (8b) gives

$$\text{VAR}(\hat{w}_0) = \frac{4\sigma_m^2 L h_m^2}{Mh^2}. \tag{23}$$

By applying the same consideration to (21), we obtain

$$\text{VAR}(\bar{w}) = \frac{4\sigma_m^2 (h/h_m)^2}{M(1 - h^2/2h_m^2)^2}\left\{\frac{e^{2\Gamma h} - 1}{2\Gamma h}\right\}. \tag{24}$$

The vertical velocity variance, normalized to $4\sigma_m^2/M$, is plotted in Fig. 15 for each of the above methods. Height increments of 1 km are assumed so that $L$ = 10 and the lapse rate of air density is $\Gamma$ = 0.113 km$^{-1}$. Although VAR($\bar{w}$) is larger than VAR($\hat{w}_0$) at 10 km, a value of $\theta_{em}$ = 40° would have resulted in VAR($\bar{w}$) being less than VAR($\hat{w}_0$) everywhere below 10 km. The direct VAD at constant range has a VAR($\hat{w}_0$) that increases without bound as $h \to 0$, because a vanishing amount of the vertical velocity contributes to the Doppler velocity. Furthermore, both direct methods have a vertical variance that increases in proportion to the height resolution (i.e., increased $L$), whereas the indirect method does not.

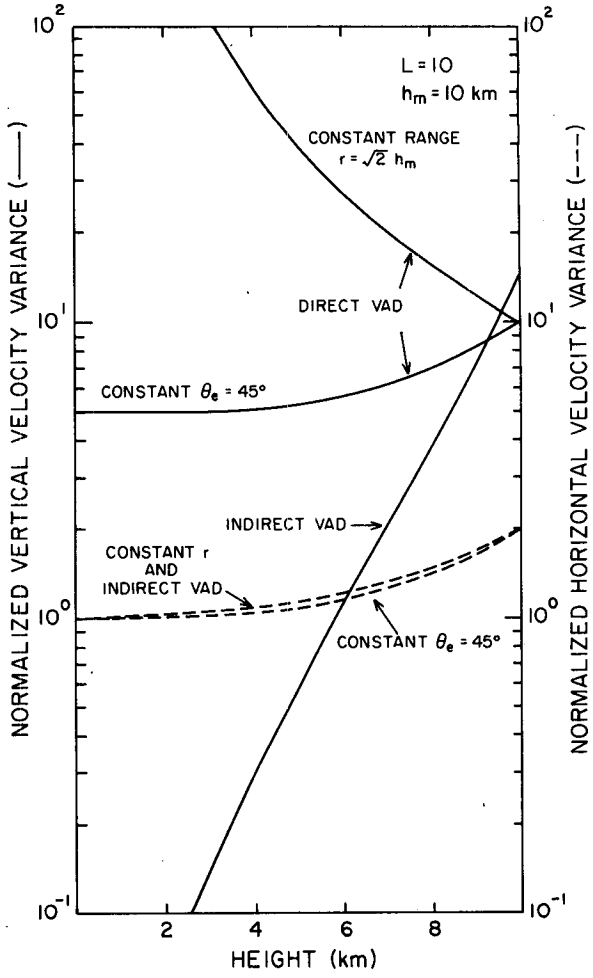


FIG. 15. The vertical (solid lines) and horizontal (dashed lines) velocity variances for three VAD techniques. Variances are normalized by the factor $\sigma_m^2/4M$.

It can also easily be shown that VAR($\hat{w}_0$) for the direct VAD at constant $\theta_{em}$ decreases as $\theta_{em}$ increases, but the indirect VAD requires a smaller maximum elevation angle to lessen VAR($\bar{w}$). Figure 15 shows that the variance in vertical velocity is larger than for the horizontal velocity but, because vertical velocity usually needs to be estimated with greater precision than the horizontal one, a variance trade-off can be made by using a higher elevation angle for the direct VAD. However, for the indirect VAD method both the vertical and horizontal wind variances decrease as $\theta_{em}$ is made smaller, so no variance trade-off is required, although height resolution will worsen due to beam divergence. Nevertheless, the indirect method offers an areal-averaged vertical velocity that requires no assumption about the spatial structure of the wind. These results suggest that the indirect method be used for estimating winds at low altitudes, whereas a direct method should be used at high altitudes.

## 5. Other considerations

Most of this analysis of profiling techniques is, of course, valid for an idealized model of flow where the large-scale wind field is linear and measurement errors are caused by small-scale turbulence and receiver noise. We have not considered the difficulty in measuring the synoptic-scale wind in the presence of wind variability associated with internal waves. Fixed beams continuously measuring the wind allow averaging of temporal variability to obtain a profile more representative of the large scales, whereas azimuth and elevation scanning allow averaging of spatial variability. When this variability is homogeneous, both samplings give equivalent estimates whose quality can be gauged from our analysis. However, nonhomogeneous variability (e.g., roll vortices, Kelvin Helmholtz waves, etc.) will produce errors that depend on factors such as range, wavelength, propagation speed etc. We have not considered these effects in this study. We also have not considered the effect of precipitation when estimates of particle fall speed are needed to derive the wind components from the radial velocities.

## 6. Summary and conclusions

We have examined the errors in three radar techniques (three fixed beams, VAD and VED) used to measure directly the three components of the wind. Equations were derived for the bias and variance of the uniform wind component estimates under the assumption of a spatially linear, time invariant wind field and a radial velocity measurement error that is a function of range. The measurement errors produce variance in the estimates and the linear wind shear biases the estimates. The variance of the estimates can be reduced by averaging more measurements but the biases cannot. Furthermore, when the radial velocity errors are dominated by the receiver noise rather than by turbulent variations in the flow, there is an optimum elevation angle of 55° for measurements of horizontal velocities. Theoretical optimum for vertical velocity measurement is 90°. Thus, for these direct measurement techniques, the selection of an elevation angle for simultaneous estimation of the three wind components requires a compromise based on the desired accuracy of the measurement.

We have also examined the errors for an indirect measurement technique based on Gauss's theorem with an equation of continuity constraint. Two advantages this indirect technique offers are that it does not depend on any assumptions about the spatial structure of the wind to measure vertical velocity and that its error variance can be smaller, because it does not require a compromise between the variances of vertical and horizontal wind components.

*Acknowledgments.* Our thanks to the reviewers for their positive criticism and encouragement, which have improved the paper, to Joy Walton and Michelle Foster for their efficient preparation of the manuscript, to Joan Kimpel for drafting the figures and to Robert Goldsmith for the photographic reductions.

APPENDIX A

### Analysis of the Fixed Beam Techniques

We wish to specify the variance and bias of the uniform wind estimates under the assumption of a spatially linear wind field. The variance of the least-squares estimates (Draper and Smith, 1981, p. 9) is given by (3). For the fixed beam technique we can evaluate $[\mathbf{P}_{nm}^T\mathbf{P}_{nm}]^{-1}$. With the assumption of spatial linearity, some or all of the derivatives can cause a bias in the uniform wind estimates, since they are not included in the model (1). For the analysis at constant height, only horizontal derivatives of the three wind components will produce bias. There are six of these but two ($u_y$, $v_x$) appear in a sum, so $l = 5$ and $\mathbf{K}_l^T = (u_y + v_x, u_x, v_y, w_z, w_y)$. With $l$ determined, the alias matrix is computed from (5).

a) For the fixed beam technique with one vertical and two off-vertical beams at elevation $\theta_e$, azimuths 0 and 90°, we find

$$\mathbf{P}_{nm} = \begin{bmatrix} \cos\theta_e & 0 & \sin\theta_e \\ & \text{[repeats } (n-N)/2 \text{ times]} & \\ 0 & \cos\theta_e & \sin\theta_e \\ & \text{[repeats } (n-N)/2 \text{ times]} & \\ 0 & 0 & 1 \\ & \text{[repeats } N \text{ times]} & \end{bmatrix} \equiv \mathbf{P}_{n3},$$

$$\mathbf{P}_{nm}^T\mathbf{P}_{nm} = \begin{bmatrix} \frac{(n-N)}{2}\cos^2\theta_e & 0 & \frac{(n-N)}{2}\cos\theta_e\cdot\sin\theta_e \\ & \frac{(n-N)}{2}\cos^2\theta_e & \frac{(n-N)}{2}\cos\theta_e\cdot\sin\theta_e \\ & & N+(n-N)\sin^2\theta_e \end{bmatrix} \equiv \mathbf{P}_3^T\mathbf{P}_3.$$

Since this is a symmetric matrix, we have not entered the identical terms below the diagonal elements. We invert $\mathbf{P}_3^T\mathbf{P}_3$ by performing a sequence of row operations to reduce it to the identity matrix. Performing this same sequence on the identity matrix reduces it to $[\mathbf{P}_3^T\mathbf{P}_3]^{-1}$ (Anton, 1981, p. 43). Thus,

$$(\mathbf{P}_3^T\mathbf{P}_3)^{-1} = \begin{bmatrix} \frac{2\sec^2\theta_e}{n-N} + \frac{\tan^2\theta_e}{N} & \frac{\tan^2\theta_e}{N} & -\frac{\tan\theta_e}{N} \\ & \frac{2\sec^2\theta_e}{n-N} + \frac{\tan^2\theta_e}{N} & -\frac{\tan\theta_e}{N} \\ & & \frac{1}{N} \end{bmatrix}, \quad \text{(A1)}$$

and, for $n = 3N$,

$$\mathrm{VAR}(\hat{u}_0) = \mathrm{VAR}(\hat{v}_0) = \frac{3\sigma_\epsilon^2}{n}(\sec^2\theta_e + \tan^2\theta_e), \quad \text{(A2)}$$

$$\mathrm{VAR}(\hat{w}_0) = \frac{3\sigma_\epsilon^2}{n}. \quad \text{(A3)}$$

To compute the alias matrix, we note that since $\phi = 0$ or 90°, the regressor variable for $(u_y + v_x)$ is always zero so it causes no bias. Thus, $l = 4$ and

$$\mathbf{P}_{nl} = \begin{bmatrix} r\cos^2\theta_e & 0 & r\cos\theta_e\cdot\sin\theta_e & 0 \\ \vdots & \vdots & \vdots & \vdots \\ 0 & r\cos^2\theta_e & 0 & r\cos\theta_e\cdot\sin\theta_e \\ \vdots & \vdots & \vdots & \vdots \\ 0 & 0 & 0 & 0 \\ \vdots & \vdots & \vdots & \vdots \end{bmatrix},$$

$\mathbf{A}_{34} = [\mathbf{P}_{nm}^T\mathbf{P}_{nm}]^{-1}\mathbf{P}_{nm}^T\mathbf{P}_{nl}$ and performing the multiplication gives

$$\mathbf{A}_{34} = \begin{bmatrix} r\cos\theta_e & & r\sin\theta_e & \\ 0 & r\cos\theta_e & 0 & r\sin\theta_e \\ 0 & 0 & 0 & 0 \end{bmatrix}.$$

Using the approximation $h \approx r\sin\theta_e$

$$\mathbf{A}_{34} = \begin{bmatrix} h\cot\theta_e & 0 & h & 0 \\ 0 & h\cot\theta_e & 0 & h \\ 0 & 0 & 0 & 0 \end{bmatrix}, \quad \text{(A4)}$$

and $\mathbf{K}_l^T = [u_x, v_y, w_x, w_y]$.

b) For the fixed beam technique with three beams at elevation $\theta_e$ and azimuths 0, 120 and 240°, we find that, for $n = 3N$,

$$\mathbf{P}_{nm} = \begin{bmatrix} \sin 0°\cdot\cos\theta_e & \cos 0°\cdot\cos\theta_e & \sin\theta_e \\ \vdots & \vdots & \vdots \\ \sin 120°\cdot\cos\theta_e & \cos 120°\cdot\cos\theta_e & \sin\theta_e \\ \vdots & \vdots & \vdots \\ \sin 240°\cdot\cos\theta_e & \cos 240°\cdot\cos\theta_e & \sin\theta_e \\ \vdots & \vdots & \vdots \end{bmatrix},$$

so therefore,

$$(\mathbf{P}_{nm}^T\mathbf{P}_{nm}) = \begin{bmatrix} \frac{n\cos^2\theta_e}{2} & 0 & 0 \\ & \frac{n\cos^2\theta_e}{2} & 0 \\ & & n\sin^2\theta_e \end{bmatrix},$$

$$(\mathbf{P}_{nm}^T\mathbf{P}_{nm})^{-1} = \begin{bmatrix} \frac{2\sec^2\theta_e}{n} & 0 & 0 \\ & \frac{2\sec^2\theta_e}{n} & 0 \\ & & \frac{\csc^2\theta_e}{n} \end{bmatrix}. \quad \text{(A5)}$$

The alias matrix can be computed as before. For this case, the regressor variable for deformation is nonzero so $l = 5$, $\mathbf{K}_l^T = [u_y + v_x, u_x, v_y, w_x, w_y]$ and

$$\mathbf{P}_{nl} = \begin{bmatrix} 0 & 0 & r\cos^2\theta_e & 0 & r\sin\theta_e\cos\theta_e \\ \vdots & \vdots & \vdots & \vdots & \vdots \\ -abr\cos^2\theta_e & a^2r\cos^2\theta_e & b^2r\cos^2\theta_e & ar\cos\theta_e\sin\theta_e & -br\sin\theta_e\cos\theta_e \\ \vdots & \vdots & \vdots & \vdots & \vdots \\ abr\cos^2\theta_e & a^2r\cos^2\theta_e & b^2r\cos^2\theta_e & -ar\cos\theta_e\sin\theta_e & -br\sin\theta_e\cos\theta_e \\ \vdots & \vdots & \vdots & \vdots & \vdots \end{bmatrix},$$

where $a = \frac{\sqrt{3}}{2}$ and $b = \frac{1}{2}$. Computing **A** as before:

$$\mathbf{A}_{35} \approx \begin{bmatrix} \frac{h\cot\theta_e}{2} & 0 & 0 & h & 0 \\ 0 & \frac{-h\cot\theta_e}{2} & 0 & 0 & \frac{h}{3} \\ 0 & \frac{h\cot^2\theta_e}{2} & \frac{h\cot^2\theta_e}{6} & 0 & \frac{h\cot\theta}{3} \end{bmatrix}. \tag{A6}$$

$$\mathbf{P}_{nm}^T\mathbf{P}_{nm} = \begin{bmatrix} \sum\cos^2\theta_e\sin^2\phi_i & \sum\cos^2\theta_e\sin\phi_i\cos\phi_i & \sum\cos\theta_e\sin\theta_e\sin\phi_i \\ & \sum\cos^2\theta_e\cos^2\phi_i & \sum\cos\theta_e\sin\theta_e\cos\phi_i \\ & & \sum\sin^2\theta_e \end{bmatrix},$$

where all summations are for $i = 1, 2, \ldots, n$. To simplify $\mathbf{P}_{nm}^T\mathbf{P}_{nm}$, we approximate the summations by integrals. For example,

$$\sum\cos^2\theta_e\sin\phi_i \approx \cos^2\theta_e\frac{n}{2\pi}\int_{-\pi}^{\pi}\sin^2\phi d\phi = \frac{n}{2}\cos^2\theta_e.$$

A similar evaluation of the remaining summations gives

$$\mathbf{P}_{nm}^T\mathbf{P}_{nm} = \begin{bmatrix} \frac{n\cos^2\theta_e}{2} & 0 & 0 \\ & \frac{n}{2}\cos^2\theta_e & 0 \\ & & n\sin^2\theta_e \end{bmatrix}.$$

$$\mathbf{P}_{nl} = r\cos\theta_e\begin{bmatrix} \cos\theta_e\cos\phi_1\sin\phi_1 & \cos\theta_e\sin\phi_1 & \cos\theta_e\cos\phi_1 & \sin\theta_e\sin\phi_1 & \sin\theta_e\cos\phi_1 \\ \cos\theta_e\cos\phi_2\sin\phi_2 & \cos\theta_e\sin\phi_2 & \cos\theta_e\cos\phi_2 & \sin\theta_e\sin\phi_2 & \sin\theta_e\cos\phi_2 \\ \vdots & \vdots & \vdots & \vdots & \vdots \\ \cos\theta_e\cos\phi_n\sin\phi_n & \cos\theta_e\sin\phi_n & \cos\theta_e\cos\phi_n & \sin\theta_e\sin\phi_n & \sin\theta_e\cos\phi_n \end{bmatrix}.$$

Performing the matrix multiplications in (5), approximating summations by integrals, and using $h \approx r\sin\theta_e$ gives

$$\mathbf{A}_{35} = \begin{bmatrix} 0 & 0 & 0 & h & 0 \\ 0 & 0 & 0 & 0 & h \\ 0 & \frac{h\cot^2\theta_e}{2} & \frac{h\cot^2\theta_e}{2} & 0 & 0 \end{bmatrix}. \tag{B3}$$

## APPENDIX C

## Analysis of the VED Technique

In the VED technique, the azimuth is fixed and the elevation angle is scanned. The range $r$ is selected for the data to be at a constant height $h$. To measure both horizontal components, another azimuth, preferably at 90° to the first, must be scanned. We assume $n/2$ data are collected for each scan. For convenience, we introduce the horizontal distance $s$, which is directed along the azimuth $\phi$. We make estimates of a horizontal component $u_0$ (directed along $s$) and the vertical component $w_0$. The regressor matrix is

$$\mathbf{P}_{nm} = \begin{bmatrix} \cos\theta_1 & \sin\theta_1 \\ \cos\theta_2 & \sin\theta_2 \\ \vdots & \vdots \\ \cos\theta_n & \sin\theta_n \end{bmatrix},$$

## APPENDIX B

## Analysis of the VAD Technique

For the VAD technique, $n$ radial velocity data are collected on a circle at height $h$. A realistic simplification is that the data are equally spaced over the circle, so

$$\mathbf{P}_{nm} = \begin{bmatrix} \cos\theta_e\sin\phi_1 & \cos\theta_e\cos\phi_1 & \sin\theta_e \\ \cos\theta_e\sin\phi_2 & \cos\theta_e\cos\phi_2 & \sin\theta_e \\ \vdots & \vdots & \vdots \\ \cos\theta_e\sin\phi_n & \cos\theta_e\cos\phi_n & \sin\theta_e \end{bmatrix},$$

Thus,

$$(\mathbf{P}_{nm}^T\mathbf{P}_{nm})^{-1} = \begin{bmatrix} \frac{2\sec^2\theta_e}{n} & 0 & 0 \\ & \frac{2\sec^2\theta_e}{n} & 0 \\ & & \frac{\csc^2\theta_e}{n} \end{bmatrix},$$

$$\mathrm{VAR}(\hat{u}_0) = \mathrm{VAR}(\hat{v}_0) = \frac{\sigma_\epsilon^2}{n}2\sec^2\theta_e, \tag{B1}$$

$$\mathrm{VAR}(\hat{w}_0) = \frac{\sigma_\epsilon^2}{n}\csc^2\theta_e. \tag{B2}$$

To find the bias caused by neglecting the linear wind field, we compute the alias matrix where $\mathbf{K}_5^T = [u_y + v_x, u_x, v_y, w_x, w_y]$:

thus,

$$\mathbf{P}_{nm}^T\mathbf{P}_{nm} = \begin{bmatrix} \sum \cos^2\theta_i & \sum \cos\theta_i \sin\theta_i \\ & \sum \sin^2\theta_i \end{bmatrix},$$

where the summations are for $i = 1, 2, \ldots, n/2$, and $\theta_i$ is the elevation angle. Approximating the summations by integrals,

$$\sum \cos^2\theta_i \approx \frac{n}{2(\pi - 2\theta_0)} \int_{\theta_0}^{\pi-\theta_0} \cos^2\theta d\theta$$

$$= \frac{n}{4}\left[\frac{(\pi - 2\theta_0) - \sin 2\theta_0}{\pi - 2\theta_0}\right]$$

$$\sum \sin\theta_i \cos\theta_i \approx 0$$

$$\sum \sin^2\theta_i \approx \frac{n}{4}\left[\frac{(\pi - 2\theta_0) + \sin 2\theta_0}{\pi - 2\theta_0}\right],$$

gives

$$(\mathbf{P}_{nm}^T\mathbf{P}_{nm})^{-1} = \begin{bmatrix} \frac{4}{n}\left[\frac{(\pi - 2\theta_0)}{(\pi - 2\theta_0) - \sin 2\theta_0}\right] & 0 \\ 0 & \frac{4}{n}\left[\frac{(\pi - 2\theta_0)}{(\pi - 2\theta_0) + \sin 2\theta_0}\right] \end{bmatrix},$$

$$\mathrm{VAR}(\hat{u}_0) = \mathrm{VAR}(\hat{v}_0) = \frac{\sigma_\epsilon^2}{n} 4\left[\frac{\pi - 2\theta_0}{(\pi - 2\theta_0) - \sin 2\theta_0}\right]$$

$$\mathrm{VAR}(\hat{w}_0) = \frac{\sigma_\epsilon^2}{n} 2\left[\frac{\pi - 2\theta_0}{(\pi - 2\theta_0) + \sin 2\theta_0}\right]. \quad \text{(C1)}$$

The variance of $w_0$ is halved because we assume that the results from the two scans will be averaged.

The bias by the linear terms is again computed from the alias matrix. The regressor variables corresponding to the excluded parameters, $\mathbf{K}_2^T = (u_s, w_s)$ are

$$\mathbf{P}_{nl} = \begin{bmatrix} r\cos^2\theta_1 & r\sin\theta_1\cos\theta_1 \\ r\cos^2\theta_2 & r\sin\theta_2\cos\theta_2 \\ \vdots & \vdots \\ r\cos^2\theta_n & r\sin\theta_n\cos\theta_n \end{bmatrix}.$$

Performing the matrix multiplications, approximating summation by integrals and using $h \approx r\sin\theta$ gives

$$\mathbf{A}_{22} = \begin{bmatrix} 0 & h \\ h\left[\frac{(\pi - 2\theta_0) - \sin 2\theta_0}{(\pi - 2\theta_0) + \sin 2\theta_0}\right] & 0 \end{bmatrix},$$

where $l = 2$ and $\mathbf{K}_l^T = [u_s, w_s]$. For the combined analysis of two scans at 0 and 90°,

$$\mathbf{A}_{34} = \begin{bmatrix} 0 & 0 & h & 0 \\ 0 & 0 & 0 & h \\ \frac{h}{2}\left[\frac{(\pi - 2\theta_0) - \sin 2\theta_0}{(\pi - 2\theta_0) + \sin 2\theta_0}\right] & \frac{h}{2}\left[\frac{(\pi - 2\theta_0) - \sin 2\theta_0}{(\pi - 2\theta_0) + \sin 2\theta_0}\right] & 0 & 0 \end{bmatrix},$$

and the vector of excluded parameters is

$$\mathbf{K}_4^T = (u_x, v_y, w_x, w_y).$$

## REFERENCES


Afifi, A. A., and S. P. Azen, 1972: *Statistical Analysis.* Academic Press, 366 pp.

Anton, H., 1981: *Elementary Linear Algebra.* Wiley, 375 pp.

Balsley, B. B., and K. S. Gage, 1982: On the use of radars for operational wind profiling. *Bull. Amer. Meteor. Soc.*, **63,** 1009–1018.

Browning, K. A., and R. Wexler, 1968: The determination of kinematic properties of a wind field using Doppler radar. *J. Appl. Meteor.*, **7,** 105–113.

Doviak, R. J., and M. Berger, 1980: Turbulence and waves in the optically clear planetary boundary layer resolved by dual-Doppler radars. *Radio Sci.*, **15,** 297–317.

——, and D. S. Zrnic', 1984: *Doppler Radar and Weather Observations.* Academic Press, 458 pp.

Draper, N. R., and H. Smith, 1981: *Applied Regression Analysis.* Wiley, 709 pp.

Koscielny, A. J., R. J. Doviak and R. Rabin, 1982: Statistical considerations in the estimation of divergence from single Doppler radar and application to prestorm boundary layer observation. *J. Appl. Meteor.*, **21,** 197–210.

Larsen, M. F., and J. Röttger, 1982: VHF and UHF Doppler radars as tools for synoptic research. *Bull. Amer. Meteor. Soc.*, **63,** 996–1008.

Peterson, V. L., and B. B. Balsley, 1979: Clear air Doppler radar measurements of the vertical component of wind velocity in the troposphere and stratosphere. *Geophys. Res. Lett.*, **6,** 933–946.

Rabin, R., and D. Zrnic', 1980: Subsynoptic-scale vertical wind revealed by dual Doppler-radar and VAD analysis. *J. Atmos. Sci.*, **37,** 644–654.

Waldteufel, P., and H. Corbin, 1979: On the analysis of single Doppler data. *J. Appl. Meteor.*, **18,** 532–542.

Zrnic', D. S., 1979: Estimation of spectral moments for weather echoes. *IEEE Trans. Geosci. Electron.*, **GE-17,** 113–128.